METEOR: Propagation of uncertainty on disaster risk analyses

Report Number: M5.4/P

10 February 2021

Contributors:
Nicole Paul
Vitor Silva

METEOR
Propagation of uncertainty on disaster risk analyses

Document Verification

Project	METEOR: Modelling Exposure Through Earth Observation Routines
Report Title	METEOR Propagation of uncertainty on disaster risk analyses
Related Milestone	M5.4
Reference as	Paul, N, Silva, V. (2021) METEOR Propagation of uncertainty on disaster risk analyses M5.4/P
Release Type	Public

Prepared by: Contributors		
Name(s): Nicole Paul Vitor Silva	Signature(s):	Date(s): 10 February 2021
Approved by: Project Manager		
Name: Kay Smith	Signature:	Date: 12 February 2021
Approved by: UKSA IPP Project Officer		
Name:	Signature:	Date:

Date	Version	Alterations	Editor

Abbreviations

Acronym	**Full Text Description**
AAL	Average Annual Losses
AALR	Average annual Loss Ratio
BGS	British Geological Survey: An organisation providing expert advice in all areas of geoscience to the UK government and internationally
DMD	Disaster Management Department: Prime Minister's Office of Tanzania focused on disaster risk
EO	Earth Observation
FATHOM	Provides innovative flood modelling and analytics, based on extensive flood risk research
GCRF	Global Challenges Research Fund
GEM	Global Earthquake Model: Non-profit organisation focused on the pursuit of earthquake resilience worldwide
GMF	Ground motion field
HOT	Humanitarian OpenStreetMap Team: A global non-profit organisation the uses collaborative technology to create OSM maps for areas affected by disasters
IM	Intensity Measure
ImageCat	International risk management innovation company supporting the global risk and catastrophe management needs of the insurance industry, governments and NGOs
IPP	International Partnership Programme
LDC	Least Developed Countriy
METEOR	Modelling Exposure Through Earth Observation Routines
NSET	National Society for Earthquake Technology: Non-governmental organisation working on reducing earthquake risk in Nepal and abroad
ODA	Official Development Assistance
OPM	Oxford Policy Management: Organisation focused on sustainable project design and implementation for reducing social and economic disadvantage in low-income

	countries
PSHA	Probabilistic Seismic Hazard Analysis
SES	Stochastic event set
UKSA	United Kingdom Space Agency
USD	US dollars currency
WP	Work Package

Contents

Figures

Tables

1. METEOR Project Introduction

1.1. Project Summary

Table 1: METEOR Project summary

Project Title	Modelling Exposure Through Earth Observation Routines (METEOR): EO-based Exposure, Nepal and Tanzania
Starting Date	08/02/2018
Duration	36 months
Partners	UK Partners: The British Geological Survey (BGS) (Lead), Oxford Policy Management Limited (OPM), SSBN Limited (Fathom) International Partners: The Disaster Management Department, Office of the Prime Minister – Tanzania (DMD), The Global Earthquake Model (GEM) Foundation, The Humanitarian OpenStreetMap Team (HOT), ImageCat, National Society for Earthquake Technology (NSET) – Nepal
Target Countries	Nepal and Tanzania for “level 2” results and all 47 Least Developed ODA countries for “level 1” data
IPP Project	IPPC2_07_BGS_METEOR

1.2. Project Overview

At present, there is a poor understanding of population exposure in some Official Development Assistance (ODA) countries, which causes major challenges when making Disaster Risk Management decisions. METEOR (Modelling Exposure Through Earth Observation Routines) takes a step-change in the application of Earth Observation exposure data by developing and delivering more accurate levels of population exposure to natural hazards.

METEOR is delivering calibrated exposure data for Nepal and Tanzania, plus “Level-1” exposure for the remaining Least developed Countries (LDCs) ODA countries. Moreover, we are: (i) developing and delivering national hazard footprints for Nepal and Tanzania; (ii) producing new vulnerability data for the impacts of hazards on exposure; and (iii) characterising how multi-hazards interact impact upon exposure. The provision of METEOR’s consistent data to governments, town planners and insurance providers will promote welfare and economic development and better enable them to respond to the hazards when they do occur.

METEOR is co-funded through the second iteration of the UK Space Agency’s (UKSA) International Partnership Programme (IPP), funded through the Global Challenges Research Fund (GCRF), which uses space expertise to deliver innovative solutions to real world problems across the globe. The funding helps to build sustainable development while building effective partnerships that can lead to growth opportunities for British companies.

1.3. Project Objectives

METEOR aims to formulate an innovative methodology of creating exposure data through the use of EO-based imagery to identify development patterns throughout a country. Stratified sampling technique harnessing traditional land use interpretation methods, modified to characterise building patterns, can be combined with EO and in-field building characteristics to capture the distribution of building types. The associated protocols and standards will be developed for broad application to ODA countries and will be tested and validated for both Nepal and Tanzania to assure they are fit-for-purpose.

Detailed building data collected on the ground for the cities of Kathmandu (Nepal) and Dar es Salaam (Tanzania) will be used to compare and validate the EO generated exposure datasets. Objectives of the project look to: deliver exposure data for 47 of the least developed ODA countries, including Nepal and Tanzania; create hazard footprints for the specific countries; create open protocols; to develop critical exposure information from EO data; and capacity-building of local decision makers to apply data and assess hazard exposure. The eight work packages (WP) that make up the METEOR project are outlined below in section 1.4.

1.4. Work Packages

Outlined below are the eight work packages that make up the METEOR project, which are led by various partners. Table 2 provides an overview of the work packages together with a brief description of what each of the work packages cover.

Table 2: Overview of METEOR work packages

Work Package	Title	Lead	Overview
WP.1	Project Management	BGS	Project management, meetings with UKSA, quarterly reporting and the provision of feedback on project deliverables and direction across primary stakeholders.
WP.2	Monitoring and Evaluation	OPM	Monitoring and evaluation of the project and its impact, using a theory of change approach to assess whether the associated activities are leading to the desired outcome.
WP.3	EO Data for Exposure Development	ImageCat	EO-based data for exposure development, methods and protocols of segmenting/classifying building patterns for stratified sampling of building characteristics.
WP.4	Inputs and Validation	HOT	Collect exposure data in Kathmandu and Dar es Salaam to help validate and calibrate the data derived from the

			classification of building patterns from EO-based imagery.
WP.5	Vulnerability and Uncertainty	GEM	Investigate how assumptions, limitations, scale and accuracy of exposure data, as well as decisions in data development process lead to modelled uncertainty.
WP.6	Multiple Hazard Impact	BGS	Multiple hazard impacts on exposure and how they may be addressed in disaster risk management by a range of stakeholders.
WP.7	Knowledge Sharing	GEM	Disseminate to the wider space and development sectors through dedicated web-portals and use of the Challenge Fund open databases.
WP.8	Sustainability and Capacity-Building	ImageCat	Sustainability and capacity-building, with the launch of the databases for Nepal and Tanzania while working with in-country experts.

1.5. Introduction to WP5: Vulnerability and Uncertainty

The consideration of uncertainty is fundamental to disaster risk assessment, both from the inherent randomness of natural phenomena (e.g. depth of rainfall in a 24-hour storm) and due to our incomplete scientific knowledge of the phenomena (e.g. lack of sufficient damage data, appropriateness of a given mathematical model). These areas of uncertainty are referred to as aleatory variability and epistemic uncertainty, respectively. Lack of consideration of these sources of uncertainty in disaster risk assessment can lead to an under- or overestimation of the risk, and consequently to erroneous decision making. Therefore, it is essential to consider different aspects of uncertainty in the various components that compose a disaster risk assessment, and propagate those through the entire process to get a full view of the range of possible outcomes. The incorporation of all sources of uncertainty in risk assessment is a fundamental goal of the METEOR project.

This report focuses on four key areas of uncertainty related to disaster risk estimates. These areas include variabilities in the hazard input, building capacity, definition of damage thresholds, and conversion of damage into an economic loss. An earlier report (referred to herein as M5.3) described these different categories of uncertainty and investigated a case study of the propagation of those uncertainties to vulnerability models, while this report will propagate a subset of those uncertainties onto the disaster risk estimates (Paul, et al. 2020).

2. Disaster risk analyses and uncertainty

Natural hazards and their impact on the built environment exhibit complex behaviour, with abundant interactions and nonlinearities that can limit our ability to predict their behaviour. In spite of this, risk due to these natural hazards should be managed and decisions must be made with a transparent assessment of uncertainties. The inherent randomness (or aleatory variability) of natural hazards is often characterised through the use of statistical models. Additionally, the incompleteness of knowledge (or epistemic uncertainty) might be characterised through the consideration of alternative models. Despite this, the complexity of the underlying behaviour of the system is only partially captured or may require further simplifications due to computational limitations (Rougier, et al., 2013) . Moreover, the disaster risk of a particular region is dynamic — a changing climate might shift the frequency and intensity of hazards, the population in a hazard-prone area may expand or contract, lack of maintenance or structural modifications might increase the vulnerability, and risk mitigation measures might be taken within a community. Further discussion of the sources of uncertainty for each considered hazard (landslides, earthquakes, floods, volcanoes) can be found in M5.3.

The effect of the propagation of uncertainties on disaster risk estimates is an active area of research within each of the natural hazard and risk disciplines (Strasser, et al., 2008; Kalakonas, et al., 2020).

3. Case study of uncertainty propagation in disaster risk analyses

3.1. Methodology

The propagation of uncertainty was performed for masonry buildings in Nepal considering earthquake ground shaking. However, the framework is generic and many takeaways equally pertain to the other natural hazards, locations, and building typologies. The four broad categories of uncertainty that were considered are summarized in Table 3.

Table 3. Categories of uncertainty considered within this study

Category	Description
Hazard input	Although singular hazard metrics are often chosen for ease of computation, there are many other factors that could influence building response. This is particularly true for dynamic hazards, such as earthquakes and landslides. This area of uncertainty is explored by using different hazard inputs with equivalent values at a given intensity level, versus considering multiple hazard inputs across a range of intensity levels.
Building-to-building	Fragility or vulnerability curves require an estimate of building capacity or strength to the hazard of interest, but robust assessment of capacity typically requires more detailed information that is available in large-scale studies. However, it is not common practice to directly consider uncertainty in these estimates. Randomly sampled capacity curves were generated based on the mean capacity curves of the considered building typologies to assess this area of variability.
Damage state threshold	Fragility curves tend to differentiate between varying degrees of damage (e.g., slight, moderate, extensive, complete). However, this requires the establishment of a damage threshold, which in reality has an inherent degree of randomness. A probabilistic distribution for this parameter was considered on this threshold to assess the implications of this uncertainty.
Loss ratio	Damage states indicate a broad state of damage (e.g., slight, moderate, extensive, complete), but the proportion of loss associated with that state is inherently random. This study investigated the use of expected loss ratios at each damage state, versus modeling a Beta distribution for each damage state.

3.2. Risk model components

3.2.1. Calculation of risk

The OpenQuake-engine was used to estimate the ground-up direct losses due to building damage. These losses are calculated using the event-based risk calculator of the OpenQuake-engine, which uses event-based Monte Carlo simulations to allow for the estimation of aggregate loss distributions for a spatially distributed portfolio of assets within a specific time period. In this process, a stochastic event set (SES) is generated to represent the seismicity of the region with the given time interval. Each event within the SES comprises an individual synthetic rupture scenario from a modelled source (consistent with the probability of occurrence provided in the model), along with an associated ground motion field (GMF) from that rupture scenario. For this study, a default of 50,000 SES were used, each with a 1-year time period in order to determine average annual losses and loss distributions. Following the derivation of GMFs for each stochastic event on its respective tectonic region type, a loss ratio is sampled for each asset within the exposure model using the vulnerability models for direct loss due to building damage. The corresponding vulnerability value (i.e. economic loss ratio) is then multiplied by the corresponding exposed value (i.e. building value in USD) to obtain the resulting risk metric (i.e. economic loss in USD).

3.2.2. Hazard model

There are several probabilistic seismic hazard analysis (PSHA) models that cover Nepal (Stevens, et al., 2018; Nath & Thingbaijam, 2012; MoPPW, 1994; Zhang, et al., 1999; Ram & Wang, 2013). For the purpose of this study, the Stevens, et. al. (2018) model was chosen due to its open availability within the timeframe of this project, in addition to the involvement of project partners of NSET in the model's development.

The two primary components of a seismic hazard model include the seismic source characterisation and the ground motion characterisation. The seismic source characterisation, or model, comprises the location, frequency, and magnitude of all possible future earthquakes that could affect the region of interest. The ground motion characterisation is used to estimate the anticipated ground shaking generated by these earthquakes, which is critical to understand the damage or risk at a given site. A depiction of the seismic source model is shown in Figure 1, and the resulting seismic hazard map is shown in Figure 2.

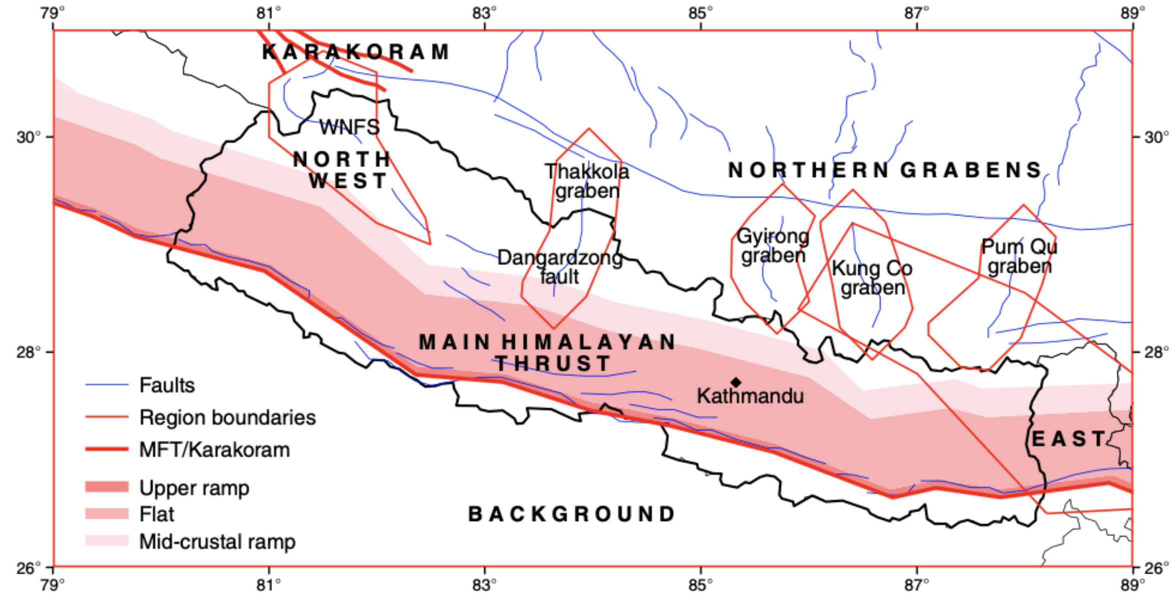

Figure 1. Seismic source characterisation within the selected hazard model for Nepal (Stevens, et al., 2018)

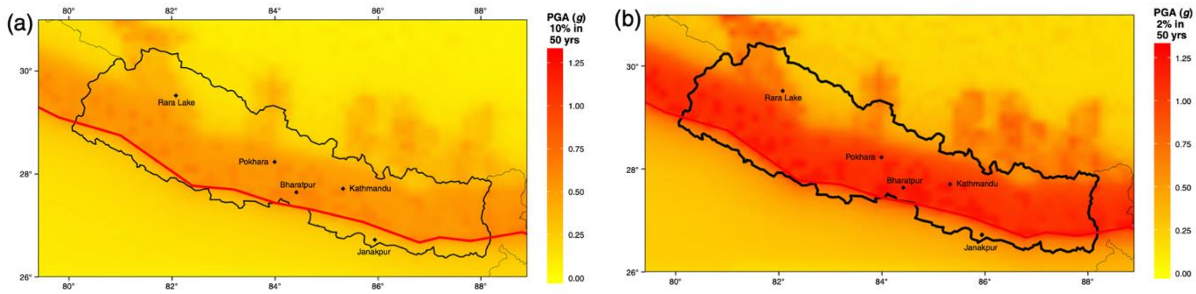

Figure 2. Seismic hazard map for Nepal using the selected hazard model for the (a) 10% in 50 year intensity level and the (b) 2% in 50 year intensity level (Stevens, et al., 2018)

Adjustments to this hazard model were made to isolate the impact of the key area of uncertainty investigated herein, which is the building-to-building variability. Those adjustments were to collapse the hazard logic tree such that there is only one ground motion prediction model per tectonic region type.

3.2.3. Exposure model

The exposure model used within this case study was the Level 3 exposure dataset for Nepal development by ImageCat within the METEOR project. Further details of the exposure development methodology can be found in deliverables M3.1 and M3.2 (ImageCat, 2018; Huyck, et al.,2019). A summary of the estimated replacement value, aggregated by municipality, is shown in Figure 3.

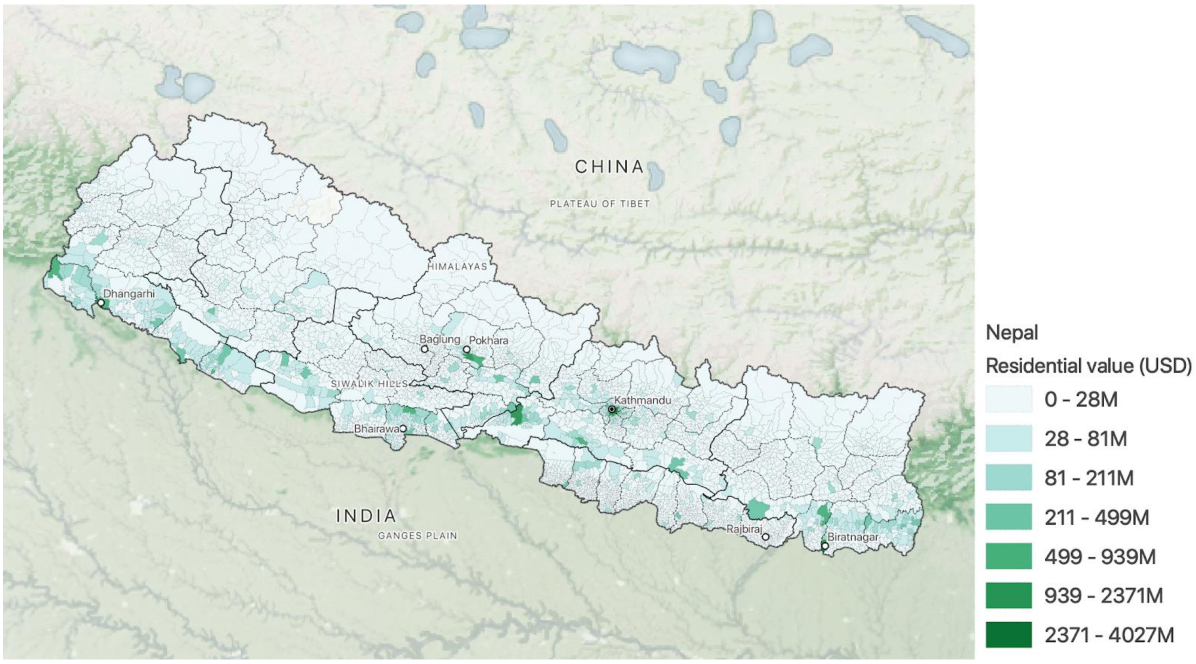

Figure 3. Value of all residential buildings in Nepal, aggregated by municipality

For the purpose of this case study, the full residential exposure model was reduced to consider only masonry buildings, for which vulnerability models with varying degrees of uncertainty propagation were derived as a part of M5.3. A summary of the estimated replacement value of masonry buildings, aggregated by municipality, is shown in Figure 4.

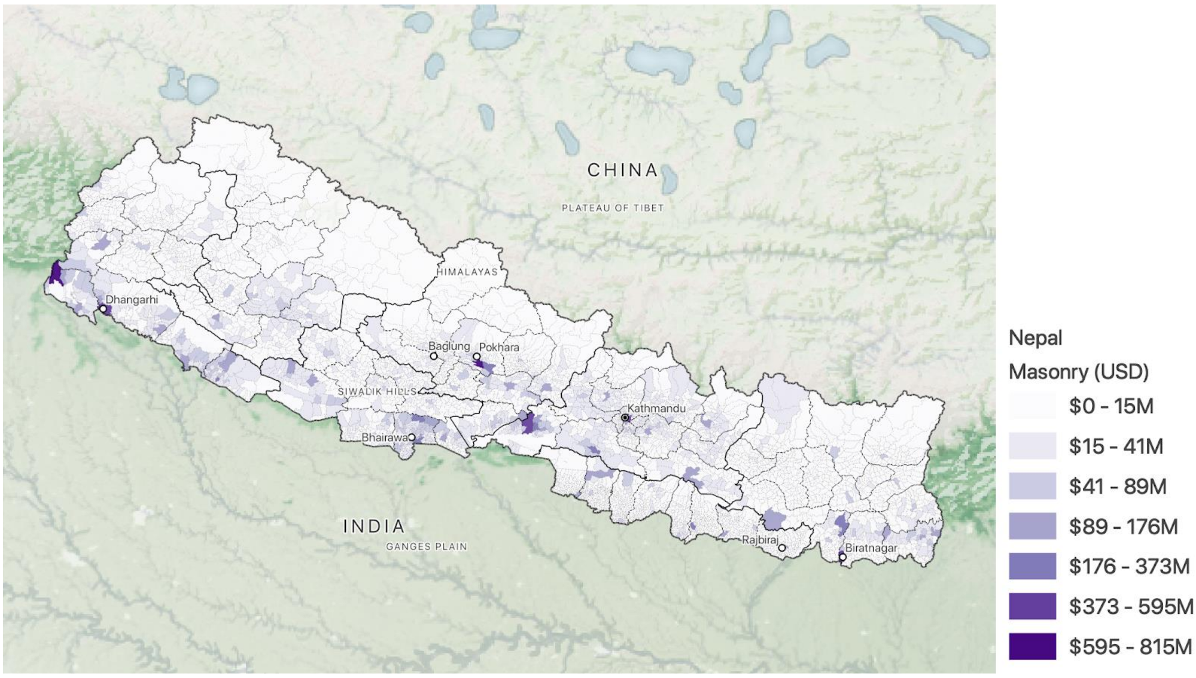

Figure 4. Value of masonry residential buildings in Nepal, aggregated by municipality

3.2.4. Vulnerability model

Fragility or vulnerability models are a fundamental component of a risk analysis model, as they relate a hazard intensity value to a probability of damage or loss, respectively. M5.3 elaborates further on fragility and vulnerability models, and also offers further technical background on the derivation of the vulnerability models used for this case study. Table 4 shows a summary of the building classes considered in this case study, for which the varying vulnerability models were derived.

Table 4. Summary of masonry building classes modelled within this study for Nepal

GEM Taxonomy	Material	Lateral system	Ductility	Stories
MUR/LWAL/DNO/H:1	Unreinforced masonry, unknown units	Wall	None	1
MUR/LWAL/DNO/H:2				2
MUR/LWAL/DNO/H:3				3
MUR/LWAL/DNO/HBET:4-5				4-5
MUR+ADO/LWAL/DNO/H:1	Unreinforced masonry, adobe blocks			1
MUR+ADO/LWAL/DNO/H:2				2
MUR+ST/LWAL/DNO/H:1	Unreinforced masonry, unknown stone			1
MUR+ST/LWAL/DNO/H:2				2
MUR+ST/LWAL/DNO/H:3				3

For the case study, the impact of building-to-building variability is of key interest. To study this, 100 statistically consistent samples of capacity curves (which underpin the vulnerability curves) were generated (see Figure 5). Each capacity curve represents a variation of a given building typology's strength and displacement capacity, and can be sent through structural analysis software to understand the estimated peak displacement in a variety of ground motions at different intensity levels. With these structural analysis results, fragility and vulnerability curves can be derived (see Figure 6 and Figure 7). Further technical details on the vulnerability derivation process can be found within M5.3.

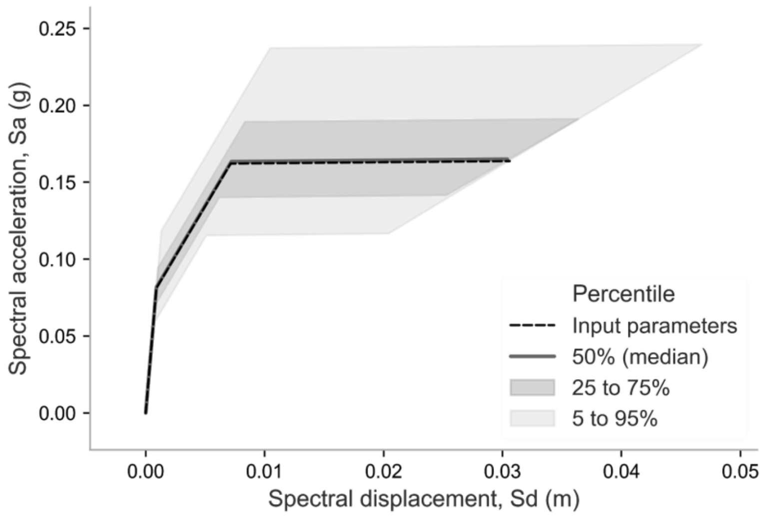

Figure 5. Comparison of resulting capacity curves from 100 random samples of MUR+ST/LWAL+DNO/H:3 in Nepal

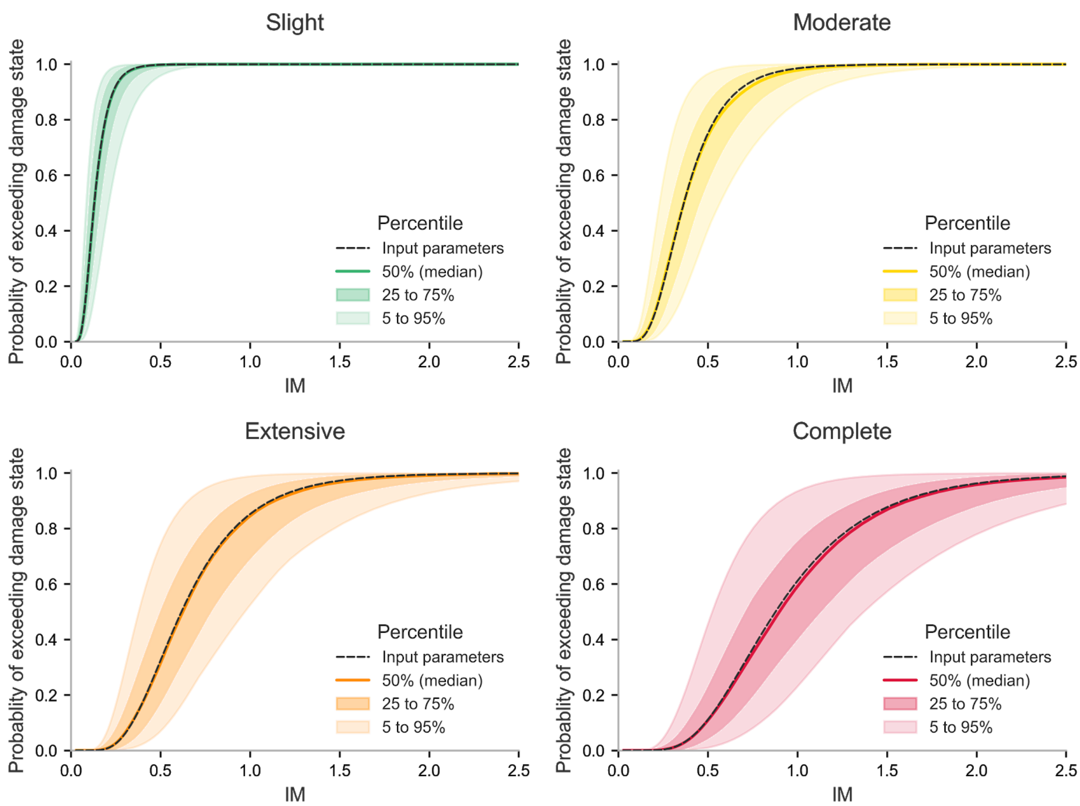

Figure 6. Comparison of resulting fragility curves from random sampling of 100 capacity curves for MUR+ST/LWAL+DNO/H:3 in Nepal

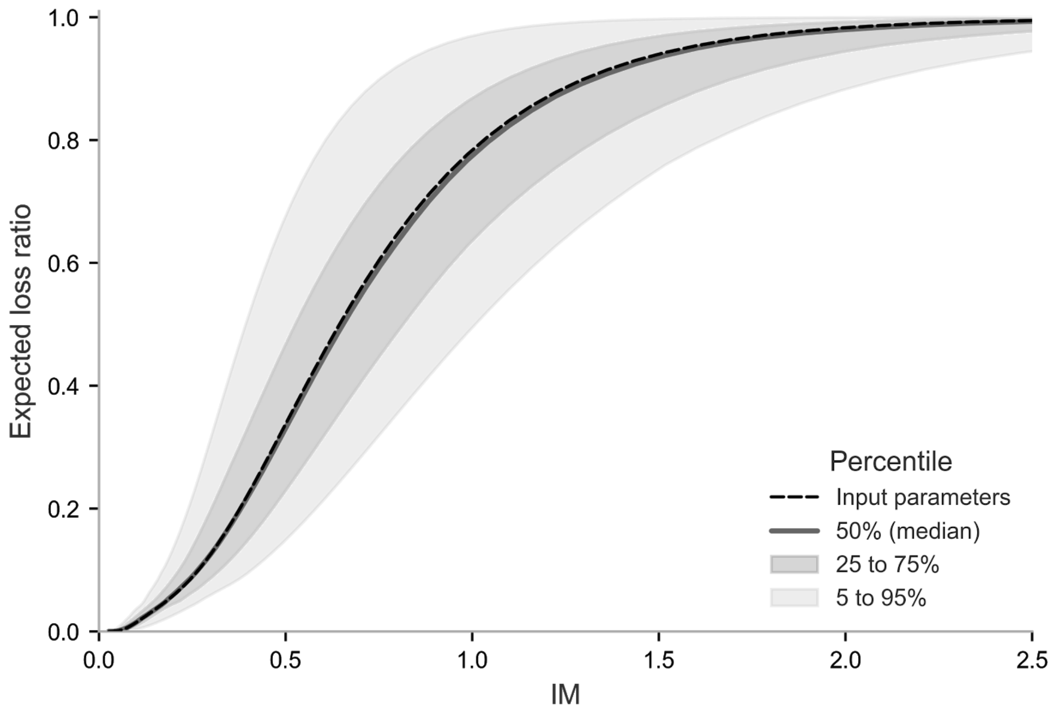

Figure 7. Comparison of resulting vulnerability curves from random sampling of 100 capacity curves for MUR+ST/LWAL+DNO/H:3 for Nepal

3.3. Evaluation of the impact of vulnerability uncertainty in disaster risk estimates

A probabilistic seismic risk assessment was run for the two model conditions (baseline case versus building-to-building variability case) per section 3.1. Key outputs of interest were the average annual losses and the loss exceedance curves.

The average annual loss (AAL) represents the expected loss averaged over a year, and the average annual loss ratio (AALR) represents that value normalised by the exposed value. Table 5 shows a summary of the comparison of AAL and AALR for the baseline case versus the building-to-building variability case for each municipality and nationally. Figure 8 shows a histogram of the percent difference between the cases across all municipalities, with the national percent difference indicated as a dashed black vertical line. Across the board, the building-to-building variability case demonstrates higher AAL and AALR values than the baseline case, ranging between 5 to 14% higher. Therefore, neglecting this aspect of uncertainty in the risk assessment would systematically bias the results and underestimate the risk.

Table 5. Summary of average annual loss (AAL), average annual loss ratio (AALR) for each municipality and nationally for each model case, and the percent difference between the two model cases for Nepal

	Average annual loss (AAL)		Average annual loss ratio (AALR)		
Municipality	Baseline	Building-to-building	Baseline	Building-to-building	Percent difference
Achham	$1,527,630	$1,643,720	0.30%	0.32%	+7.60%
Arghakhanchi	$1,561,450	$1,674,940	0.32%	0.35%	+7.27%
Baglung	$1,714,980	$1,871,520	0.25%	0.27%	+9.13%
Baitadi	$1,923,880	$2,086,490	0.29%	0.31%	+8.45%
Bajhang	$829,345	$914,017	0.22%	0.24%	+10.21%
Bajura	$641,138	$707,481	0.25%	0.28%	+10.35%
Banke	$6,129,470	$6,676,240	0.34%	0.37%	+8.92%
Bara	$2,685,620	$2,991,320	0.27%	0.30%	+11.38%
Bardiya	$3,625,830	$3,917,760	0.36%	0.39%	+8.05%
Bhaktapur	$1,559,990	$1,738,500	0.41%	0.46%	+11.44%
Bhojpur	$857,138	$930,034	0.29%	0.31%	+8.50%
Chitawan	$14,208,600	$15,246,800	0.74%	0.79%	+7.31%
Dadeldhura	$1,191,430	$1,290,360	0.31%	0.33%	+8.30%
Dailekh	$1,656,330	$1,780,370	0.35%	0.38%	+7.49%
Dang	$6,685,440	$7,077,800	0.55%	0.58%	+5.87%
Darchula	$643,020	$717,984	0.17%	0.19%	+11.66%
Dhading	$2,325,120	$2,543,700	0.25%	0.28%	+9.40%
Dhankuta	$831,439	$905,551	0.28%	0.30%	+8.91%
Dhanusa	$2,455,470	$2,762,310	0.22%	0.25%	+12.50%
Dolakha	$1,818,740	$2,005,950	0.23%	0.26%	+10.29%
Dolpa	$77,564	$88,478	0.09%	0.10%	+14.07%
Doti	$1,215,350	$1,311,510	0.30%	0.32%	+7.91%
Gorkha	$2,166,350	$2,367,080	0.26%	0.28%	+9.27%
Gulmi	$2,417,440	$2,619,830	0.29%	0.31%	+8.37%
Humla	$310,128	$340,687	0.24%	0.26%	+9.85%
Ilam	$1,397,270	$1,519,350	0.27%	0.29%	+8.74%
Jajarkot	$1,522,900	$1,668,480	0.25%	0.28%	+9.56%
Jhapa	$4,714,200	$5,125,020	0.36%	0.39%	+8.71%
Jumla	$811,809	$881,489	0.30%	0.32%	+8.58%
Kailali	$5,605,840	$6,151,620	0.36%	0.40%	+9.74%
Kalikot	$573,294	$629,693	0.25%	0.28%	+9.84%
Kanchanpur	$7,235,080	$7,892,980	0.44%	0.48%	+9.09%
Kapilbastu	$4,213,400	$4,573,680	0.36%	0.39%	+8.55%
Kaski	$7,117,410	$7,893,720	0.37%	0.41%	+10.91%
Kathmandu	$5,401,070	$6,147,200	0.39%	0.45%	+13.81%
Kavrepalanchok	$5,042,170	$5,443,180	0.37%	0.40%	+7.95%
Khotang	$725,961	$788,982	0.28%	0.30%	+8.68%

Lalitpur	$3,394,790	$3,747,890	0.38%	0.42%	+10.40%
Lamjung	$1,080,400	$1,195,750	0.21%	0.24%	+10.68%
Mahottari	$1,705,010	$1,923,790	0.20%	0.23%	+12.83%
Makwanpur	$4,945,250	$5,399,200	0.41%	0.45%	+9.18%
Manang	$21,323	$24,024	0.10%	0.11%	+12.66%
Morang	$3,409,800	$3,777,960	0.25%	0.28%	+10.80%
Mugu	$278,203	$307,522	0.25%	0.27%	+10.54%
Mustang	$61,216	$68,454	0.10%	0.11%	+11.82%
Myagdi	$827,543	$906,405	0.22%	0.24%	+9.53%
Nawalparasi	$7,192,510	$7,763,300	0.46%	0.50%	+7.94%
Nuwakot	$2,081,320	$2,290,630	0.24%	0.26%	+10.06%
Okhaldhunga	$1,105,000	$1,203,920	0.28%	0.30%	+8.95%
Palpa	$1,928,520	$2,084,160	0.31%	0.33%	+8.07%
Panchthar	$879,464	$958,621	0.28%	0.30%	+9.00%
Parbat	$1,168,710	$1,274,000	0.27%	0.29%	+9.01%
Parsa	$1,370,550	$1,555,310	0.23%	0.26%	+13.48%
Pyuthan	$1,316,580	$1,422,780	0.28%	0.30%	+8.07%
Ramechhap	$2,218,240	$2,432,040	0.26%	0.29%	+9.64%
Rasuwa	$219,737	$243,688	0.19%	0.21%	+10.90%
Rautahat	$1,813,580	$2,015,720	0.23%	0.25%	+11.15%
Rolpa	$1,714,110	$1,863,440	0.26%	0.29%	+8.71%
Rukum	$1,807,840	$1,981,700	0.24%	0.26%	+9.62%
Rupandehi	$10,446,400	$11,517,400	0.34%	0.38%	+10.25%
Salyan	$1,674,360	$1,811,490	0.30%	0.32%	+8.19%
Sankhuwasabha	$711,798	$782,035	0.27%	0.30%	+9.87%
Saptari	$1,657,800	$1,817,480	0.29%	0.32%	+9.63%
Sarlahi	$2,619,140	$2,895,740	0.28%	0.31%	+10.56%
Sindhuli	$2,195,080	$2,395,820	0.29%	0.32%	+9.15%
Sindhupalchok	$2,960,160	$3,246,480	0.25%	0.28%	+9.67%
Siraha	$2,037,080	$2,252,940	0.30%	0.33%	+10.60%
Solukhumbu	$659,901	$731,836	0.22%	0.25%	+10.90%
Sunsari	$4,068,440	$4,479,060	0.39%	0.43%	+10.09%
Surkhet	$2,306,620	$2,481,560	0.34%	0.37%	+7.58%
Syangja	$2,091,190	$2,275,340	0.30%	0.33%	+8.81%
Tanahu	$3,795,050	$4,132,710	0.36%	0.39%	+8.90%
Taplejung	$704,706	$781,787	0.25%	0.28%	+10.94%
Terhathum	$617,976	$673,610	0.27%	0.30%	+9.00%
Udayapur	$1,575,860	$1,709,370	0.40%	0.44%	+8.47%
National	$186,081,000	$203,351,000	0.33%	0.36%	+9.28%

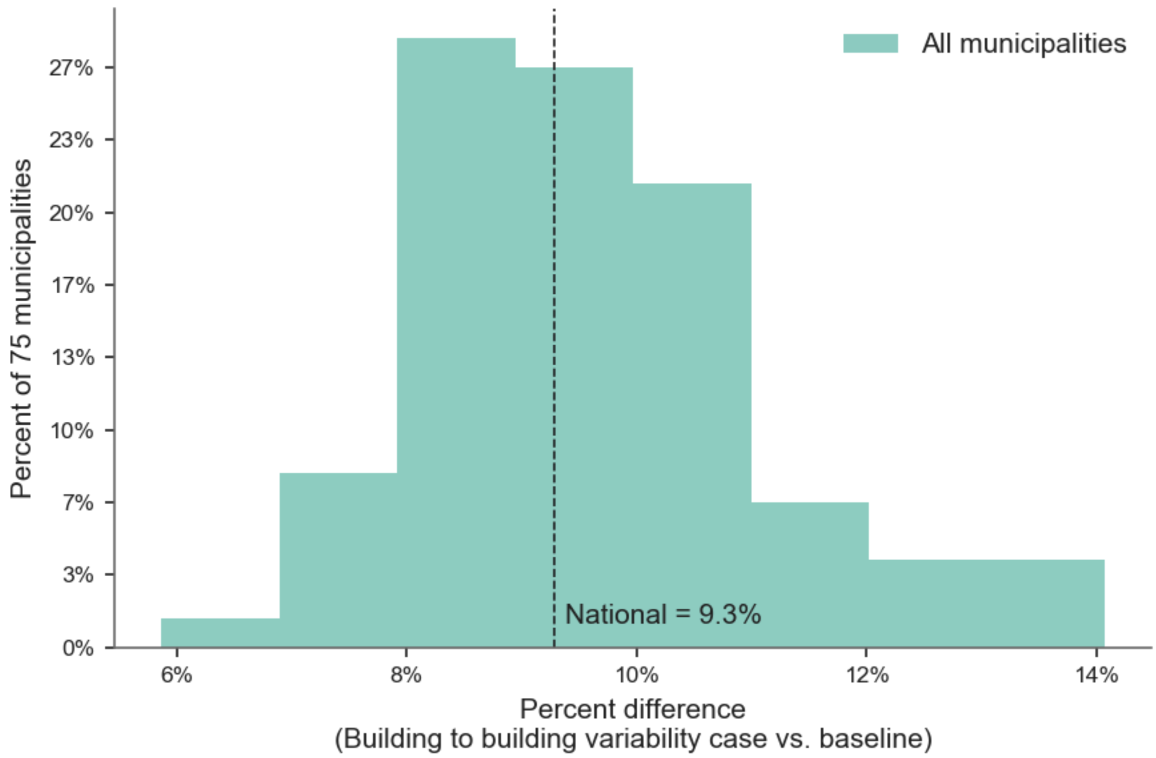

Figure 8. Histogram of percent difference in average annual loss (AAL) or average annual loss ratio (AALR) between the two model cases across all municipalities in Nepal, with the national percent difference indicated as a dashed black vertical line

Loss exceedance curves are defined as the aggregate loss expected to be exceeded at a given return period. Table 6 summarises the national loss exceedance curves for the baseline case versus the building-to-building variability case. Figure 9 depicts the percent difference of those results in a thick black curve, along with the percent difference at each municipality as a thin green curve.

Table 6. National loss exceedance curves for each model case and the percent difference between the two cases

Return period	Baseline model	Building-to-building variability	Percent Difference
5	$142M	$158M	+11.2%
10	$284M	$311M	+9.5%
20	$554M	$585M	+5.7%
50	$1,226M	$1,273M	+3.9%
100	$2,181M	$2,219M	+1.7%
200	$3,544M	$3,608M	+1.8%
500	$6,648M	$6,740M	+1.4%
1,000	$9,180M	$9,173M	-0.1%

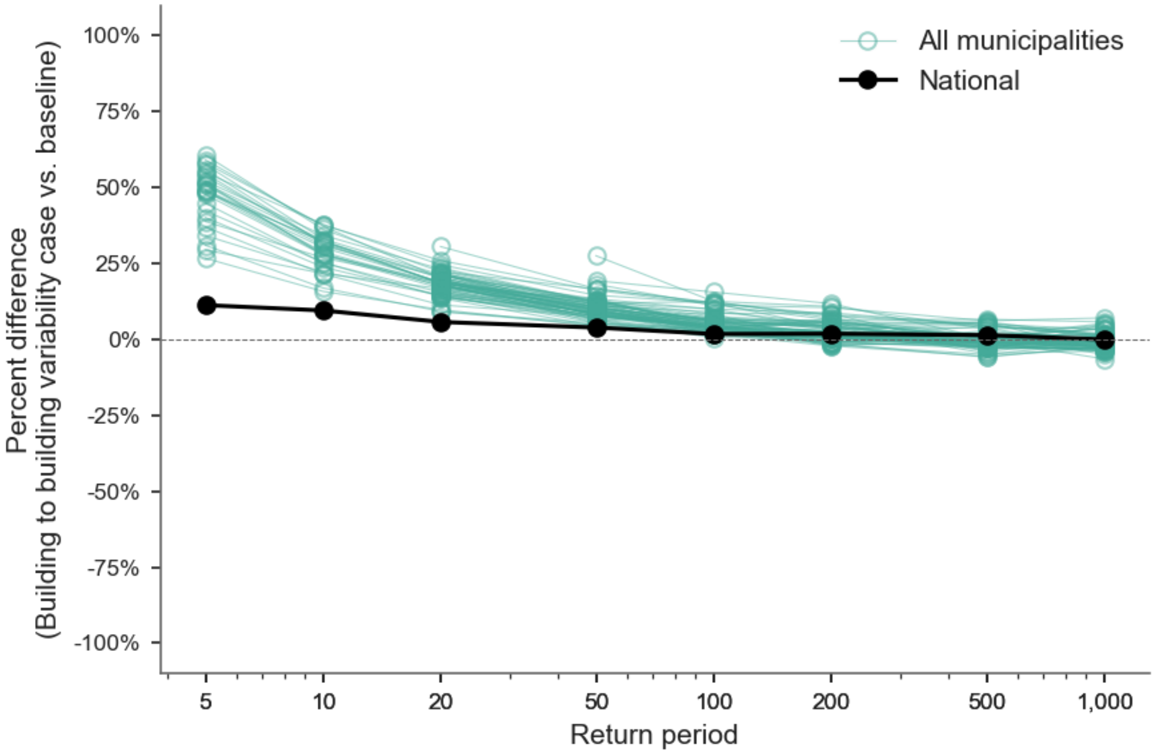

Figure 9. Percent difference in loss exceedance curves across all municipalities in Nepal, with the national percent difference indicated as a thick black curve

The results reveal a trend where the building-to-building variability case has more significantly different (and higher) loss results at lower return periods, but that the percent difference decreases as the return periods increase. Moreover, at the highest considered return period (1,000 year), the building-to-building variability case even has slightly lower loss results than the baseline case. This result can be explained by the difference in the mean vulnerability curves that resulted from the analysis performed as a part M5.3, as can be seen in Figure 10. The consideration of building-to-building variability through explicit modelling of alternate building capacity curves yields a range of fragility or vulnerability curve outcomes, and the average fragility or vulnerability curve across that set of analyses becomes "flatter" relative to the baseline case (i.e. without consideration of varying building capacity curves). This means that there is a larger proportion of damage at lower hazard intensity levels, but also a lesser proportion of damage at higher intensity levels for the building-to-building variability case. Therefore, at lower return periods (which yield lower hazard intensities), there is more significant damage and loss for the building-to-building case than the baseline case. Yet, at the higher return periods (which yield higher hazard intensities), this percent difference drops off and even trends in the opposite direction (i.e. lesser damage and loss). Since the lower return periods (or lower hazard intensity levels) are more frequent, they contribute more to the AAL or AALR relative to the higher return periods (or higher intensity levels). This explains why the AAL or AALR of the building-to-building variability case was consistently higher than the baseline case, as discussed previously.

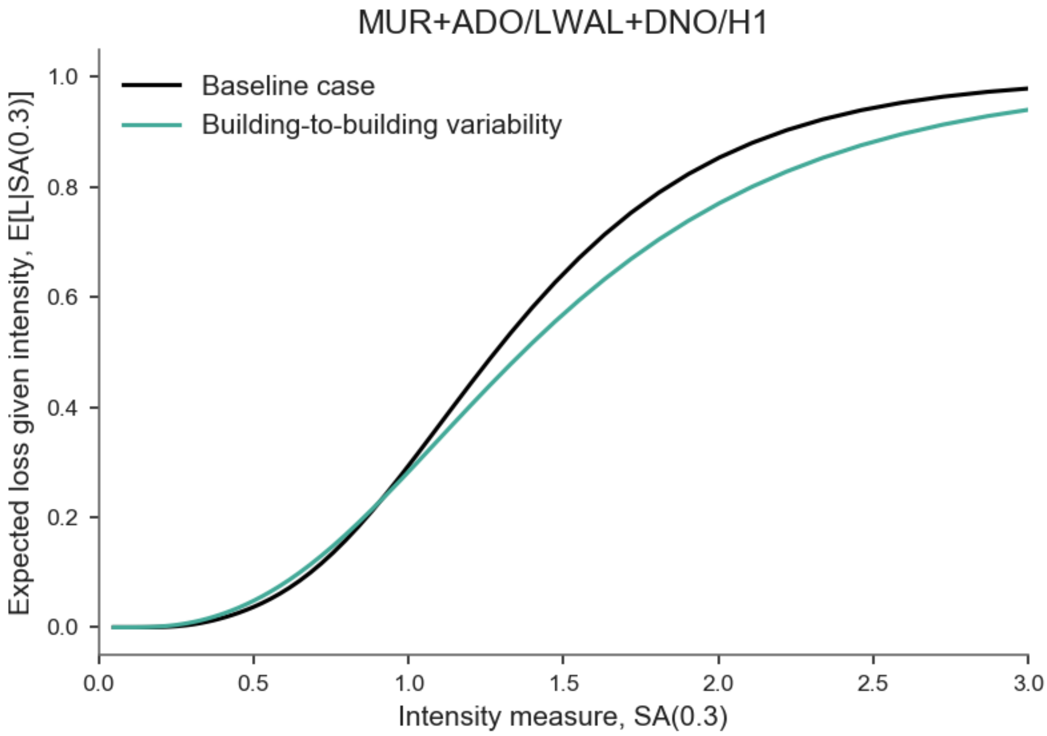

Figure 10. Comparison of mean vulnerability curves for MUR+ADO/LWAL+DNO/H:1 building class in Nepal between the two model cases

4. Discussion

This study shows that a failure to propagate the uncertainty in vulnerability models to the disaster risk analysis can systematically bias the results in a manner that is unconservative. Within the METEOR project, special attention was devoted to the development of detailed exposure datasets at the national scale, which covers a wide range of buildings classes, and each class will naturally comprise buildings with varying geometrical and material properties. It is thus fundamental to account for this source of aleatory uncertainty in the vulnerability component of the risk analyses. The results presented in section 3.3 (which use the vulnerability functions described in the previous deliverable), indicate a consistent underestimation of the risk metrics for frequent events (and consequently on the average annual losses and losses for short return periods), and a slightly over estimation for rare return periods.

Bibliography

Huyck, C., P. Hu, G. Amyx, M. Esquivias, M. Huyck, and M. Eguchi. 2019. "METEOR: Exposure Data Classification, Metadata Population, and Confidence Assessment." Report M3.2/P.

ImageCat. 2018. "Draft Taxonomy and Data Model: Structure and Scale." Report Number: M3.1/C.

Kalakonas, P., A. Rao, A. Mouyiannou, and V. Silva. 2020. "Exploring the Impact of Epistemic Uncertainty on Regional Probabilistic Seismic Risk Asessment." *Natural Hazards* 104 (1): 997-1020.

MoPPW. 1994. "NBC 105: Nepal National Building Code." Babar Mahal, Kathmandu, Nepal.

Nath, S. K., and K. K. S. Thingbaijam. 2012. "Probabilistic seismic hazard assessment of India." *Seismological Research Letters* 83 (1): 135-149.

Paul, N., V. Silva, R. Guragain, S. Wagle, and S. Shrestha. 2020. "METEOR Assessment of Vulnerability Uncertainty." Report M5.3/C.

Ram, Thapa Dili, and Guoxin Wang. 2013. "Probabilistic seismic hazard analysis in Nepal." *Earthquake Engineering and Engineering Vibration* 12: 577-586.

Rougier, Jonathan, Lisa J. Hill, and Robert Stephen John Sparks. 2013. *Risk and uncertainty assessment for natural hazards.* Cambridge Univesity Press.

Stevens, V. L., S. N. Shrestha, and D. K. Maharjan. 2018. "Probabilistic Seismic Hazard Assessment of Nepal." *Bulletin of the Seismological Society of America* 108 (6): 3488-3510.

Strasser, F. O., J. J. Bommer, K. Sesetyan, M. Erdik, Z. Cagnan, J. Irizarry, X. Goula, et al. 2008. "A comparative study of European earthquake loss estimation tools for an earthquake scenario in Istanbul." *Journal of Earthquake Engineering* 12 (S2): 246-256.

Zhang, Peizhen, Zhi-xian Yang, Harsh K. Gupta, Satish C. Bhatia, and Kaye M. Shedlock. 1999. "Global seismic hazard assessment program (GSHAP) in continental Asia." *Annali di Geofisica* 42 (6): 1167-1190.